Simultaneous Feeder Reconfiguration and Distributed Generation Planning in the Presence of Voltage-Dependent and Variable Loads

Meisam Mahdavi and Augustine Awaafo
Department of Electrical Engineering
University of Jaen
Linares, Jaen, Spain
mmahdavi@ujaen.es; aa000145@red.ujaen.es

Mohsen Dini
GE Power Conversion
Villebon, France
mohsen.dini@ge.com

Siamak Moradi
SYD Power Electrical Company
Sydney, Australia
info@sydpowerelectrical.com

Francisco Jurado and David Vera
Department of Electrical Engineering
University of Jaen
Linares, Jaen, Spain
fjurado@ujaen.es; dvera@ujaen.es

***Abstract*—In distribution systems, where distribution losses and the output of distributed generators (DGs) are significantly impacted by load power, an effective approach for reducing power loss is required, which the hybrid operation of DG units and grid reconfiguration can serve as a best alternative. Load power exhibits variability, altering alongside the voltage fluctuations which occur over time. Furthermore, the correlation between power demand and voltage relies on the type of load. Nonetheless, the incorporation of these important concerns into research on reconfiguration and distributed generation planning is rare. Only a limited number of papers have taken into account the voltage dependence and the type of time-varying loads in their respective models. Nevertheless, they proposed models with significant nonlinearity, requiring computation through nonlinear solvers or metaheuristic algorithms. Meanwhile, these models require the use of intensive linearization techniques to facilitate their implementation through linear solvers. High computational time is demanded by nonlinear solvers, while metaheuristic algorithms cannot guarantee the attainment of optimal solutions. Hence, the accurate modeling of load behavior holds importance in the active distribution system reconfiguration. In this paper, a proficient reconfiguration model is presented, which is both straightforward for implementation in conventional optimization tools and adept at identifying appropriate solutions for the reconfiguration and DG planning problem.**

***Index Terms*—Distributed generation planning, distribution systems, efficient load modeling, voltage dependency.**

I. INTRODUCTION

In the context of modern power systems the reduction of power losses in distribution grids is a significant concern, which can be achieved by the involvement of reconfiguration and distributed generators (DGs) in the power planning architecture [1]-[3]. This can mitigate the substantial impact of losses on power quality and efficiency reduction. In reconfiguration and DG allocation, the grid topology is adjusted in the presence of distributed generators for a given load level. This adjustment involves the manipulation of sectional and tie-line switches, achieved by opening and closing them [4], [5]. Due to variations in time and voltage, the load power undergoes changes, consequently impacting power losses and the output of distributed generators. Numerous models have been introduced to address the challenge associated with distribution system reconfiguration when incorporating DG. Unfortunately, a substantial majority of these models have overlooked the voltage-dependent nature of loads within their formulations. On the other hand, a limited number of studies that integrated voltage-dependent loads into their models introduced nonlinear formulations, which has been handled by metaheuristic algorithms. However, they do not provide an assurance of optimal solutions. These models might require subsequent computation by nonlinear solvers following intensive computational processes. Therefore, creating a reconfiguration model that is compatible with linear solvers would be beneficial for both distribution system operators and researchers.

In the presence of distributed generation, a new metaheuristic optimization technique, named teaching-learning-based optimization (TLBO) algorithm was employed in [6] for loss reduction and voltage profile improvement using grid reconfiguration. Although the TLBO performance is better than particle swarm optimization (PSO), metaheuristics cannot ensure the optimal solutions in large-scale systems. Thus, in [7], mixed-integer quadratic programming (MIQP) based on linear branch flow equations was developed for formulating the reconfiguration problem in the presence of distributed generators. In spite of the highly efficient implementation of the proposed method in classic optimization platforms, linearization and approximations used in the linear branch flow model decreases the performance of the reconfiguration approach presented in [7].

The search group algorithm (SGA) was developed in [8] to reconfigure radial distribution systems connected to DG units. Nevertheless, a chaotic local search strategy was employed to improve the SGA search ability by preventing the algorithm trapping in local minima. This shows an unreliable performance of search group algorithm in approaching accurate solutions for large distribution grids.

In [9], the grid reconfiguration was performed considering distributed generation using a parallel slime mould algorithm (PSMA) for reducing power losses, enhancing voltage stability, mitigating load unbalances, and identifying time of switching. The PSMA method, utilizing a grouping communication strategy and an inertia weight, demonstrates superior performance when compared to both the whale optimization algorithm (WOA) and the adaptive WOA (AWOA). In [10], DG was used to minimize power losses in the reconfigurable distribution systems, employing both ant colony optimization (ACO) and ant search (AS) techniques. It was shown that considering DGs' power during reconfiguration leads to the achievement of lower system losses. However, the optimal solutions cannot be guaranteed by metaheuristics like PSMA, AS, and ACO. Lastly, in [11], a self-adaptive firework algorithm (SAFWA) and iterative game theory were employed in a market-based reconfiguration to determine locational marginal prices (LMPs) at buses connected to distributed generators. However, in [11] and all the previously reviewed models, the voltage dependency of loads has been disregarded, despite its significance in simultaneous reconfiguration and DG utilization.

To address this, [12] introduced a mixed-integer linear programming (MILP) model, utilizing a mathematical programming language (AMPL), for solving the reconfiguration problem in the presence of DG and voltage-dependent loads. In this model, piecewise linear functions were employed to approximate all nonlinear terms and quadratic equations describing the dependence of load power on voltage. However, it is worth noting that the high degree of simplification and approximation of quadratic equations in [12] may potentially compromise the efficiency of the proposed model, particularly when applied to the reconfiguration of large distribution systems. In [13], a mixed-integer nonlinear programming (MNLP) model was introduced to address this issue by considering distributed generators and the voltage dependency of loads in solving the reconfiguration problem. Nevertheless, the computational demands of the model proposed in [13], when utilizing nonlinear solvers, are substantial, rendering it unsuitable for reconfiguring medium- and large-sized distribution grids. Therefore, in [14], a genetic algorithm (GA) was utilized to address the reconfiguration problem, incorporating various types of voltage-variant loads and distributed generators. However, it should be noted that the standard GA method is time-consuming when applied to reconfiguration applications. In [15], the reconfiguration of the distribution system was investigated, taking into account voltage-dependent loads and volt-var control devices, and it was tackled using the gray wolf optimization (GWO) method. Nonetheless, it is essential to acknowledge that, approaches relying on metaheuristic algorithms cannot assure optimal or precise solutions, especially in large-scale reconfiguration problems. Therefore, in [16], the general algebraic modeling system (GAMS) was utilized to address the reconfiguration problem while accounting for demand response and the voltage dependency of responsive loads in the presence of distributed generation. However, it is important to note that dealing with uncertainties related to demand and DG power through Monte Carlo simulation (MCS) can be computationally intensive.

Finally, in [17], the simultaneous planning and reconfiguration of active distribution systems were addressed, incorporating considerations of carbon dioxide (CO_2) emissions and voltage-dependent loads. The utilization of AMPL in this context was employed. The results of the study show that integrating grid reconfiguration into the planning problem leads to reduced operational and planning costs [18], as well as decreased CO_2 pollution. Nevertheless, the nonlinear models presented in [6], [8]–[11], and [13]-[15] necessitated that the computation be done through commercial nonlinear solvers, entailing time-consuming processes or via metaheuristic algorithms that could not guarantee optimal solutions. Additionally, the use of extensive linearization and numerous approximations in [7], [12], [16], and [17] resulted in less precise linear reconfiguration and DG planning models. It is important to emphasize that the use of the linearization technique should not significantly compromise the precision of the models. Conversely, employing metaheuristic algorithms to solve nonlinear models does not assure precise solutions and typically entails time-consuming computations in conventional optimization tools. Therefore, this paper introduces an efficient model for addressing reconfiguration problems in the presence of distributed generation and voltage-dependent loads. This model leverages commercial linear solvers, eliminating the requirement for extensive linearization and approximation. Therefore, the main contributions and novelties of the paper are:

- Suggestion of a linear model for simultaneous feeder reconfiguration and DG planning problem in the presence of nonlinear voltage-dependent loads without extensive linearization and approximation.
- Development of a voltage-reliant reconfiguration model in the presence of distributed generators that can be easily computed by linear solvers as opposite to nonlinear models.
- Attainment of exact solutions in short computational time compared to metaheuristic and nonlinear approaches.

II. Modeling the Relationship Between Power Consumption, Time, and Voltage

Depending on the load type, active and reactive demands react differently to voltage variations in the distribution system. For example, the dependence of computers on voltage magnitude is lower than that of fluorescent lamps. Using the exponential model, the dependency of load powers on voltage, time, and consumer type can be represented as follows [19].

$$Pd_i(t) = Pd_i^n(t)\left(V_i(t)/V_n\right)^{\alpha} \tag{1}$$

$$Qd_i(t) = Qd_i^n(t)\left(V_i(t)/V_n\right)^{\beta} \tag{2}$$

Where, active and reactive loads as well as voltage magnitude at load point i and time t are exhibited by $Pd_i(t)$, $Qd_i(t)$, and $V_i(t)$, in which their nominal values are shown by $Pd_i^n(t)$, $Qd_i^n(t)$, and V_n, respectively. Also, the active and reactive load exponents are illustrated by α and β, respectively. However, each bus of real distribution systems is connected to different types of loads. Therefore, a general representation can be expressed for (1) and (2) as

$$Pd_i(V_i(t), y) = Pd_i^n(t)\sum\nolimits_y A_y\left(V_i(t)/V_n\right)^{\alpha_y} \tag{3}$$

$$Qd_i(V_i(t), y) = Qd_i^n(t)\sum\nolimits_y B_y\left(V_i(t)/V_n\right)^{\beta_y} \tag{4}$$

In (3) and (4), the active and reactive power exponents of load type y are denoted as α_y and β_y, respectively. Exponent values should be determined by the network operator for any case study system regarding the behavior of the specific loads, especially in today's power systems which have different load behaviors due to technological advancement. Therefore, the coefficients will properly be estimated with a large variance in practice that affects load amount and subsequent obtained solutions. It should be noted that this issue does not affect the performance of the algorithm suggested in current research because the proposed model is a generalized formulation that can include any type of loads with different coefficients. A_y and B_y coefficients represent the percentages of active and reactive load types connected to each consumption point, respectively, that should be

$$\sum_y A_y = \sum_y B_y = 1 \tag{5}$$

Equations (6) and (7) could be attained by adding and subtracting 1 to/from (3) and (4).

$$Pd_i(V_i(t), y) = Pd_i^n(t) \sum_y A_y \left(1 + V_i(t)/V_n - 1\right)^{\alpha_y} \tag{6}$$

$$Qd_i(V_i(t), y) = Qd_i^n(t) \sum_y B_y \left(1 + V_i(t)/V_n - 1\right)^{\beta_y} \tag{7}$$

Equations (6) and (7) can be rewritten as follows using the binomial theorem, considering that the voltage magnitudes of load points in distribution systems are close to the nominal voltage.

$$\begin{aligned} Pd_i(V_i(t), y) &= Pd_i^n(t) \sum_y A_y + Pd_i^n(t) \sum_y A_y \alpha_y \left(V_i(t)/V_n - 1\right) \\ &+ 1/2\, Pd_i^n(t) \sum_y A_y \alpha_y \left(\alpha_y - 1\right)\left(V_i(t)/V_n - 1\right)^2 \\ &+ 1/6\, Pd_i^n(t) \sum_y A_y \alpha_y \left(\alpha_y - 1\right)\left(\alpha_y - 2\right)\left(V_i(t)/V_n - 1\right)^3 + \ldots \end{aligned} \tag{8}$$

$$\begin{aligned} Qd_i(V_i(t), y) &= Qd_i^n(t) \sum_y B_y + Qd_i^n(t) \sum_y B_y \beta_y \left(V_i(t)/V_n - 1\right) \\ &+ 1/2\, Qd_i^n(t) \sum_y B_y \beta_y \left(\beta_y - 1\right)\left(V_i(t)/V_n - 1\right)^2 \\ &+ 1/6\, Qd_i^n(t) \sum_y B_y \beta_y \left(\beta_y - 1\right)\left(\beta_y - 2\right)\left(V_i(t)/V_n - 1\right)^3 + \ldots \end{aligned} \tag{9}$$

Due to grid security issues, the voltage magnitude of each bus is limited to vary within a small range of nominal voltage in distribution system reconfiguration. Therefore, $|1 - V_i(t)/V_n| << 1$ and following quadratic expressions can efficiently approximate (8) and (9).

$$\begin{aligned} Pd_i(V_i(t), y) &\cong Pd_i^n(t) \sum_y A_y + Pd_i^n(t) \sum_y A_y \alpha_y \left(V_i(t)/V_n - 1\right) \\ &+ 1/2\, Pd_i^n(t) \sum_y A_y \alpha_y \left(\alpha_y - 1\right)\left(V_i(t)/V_n - 1\right)^2 \end{aligned} \tag{10}$$

$$\begin{aligned} Qd_i(V_i(t), y) &\cong Qd_i^n(t) \sum_y B_y + Qd_i^n(t) \sum_y B_y \beta_y \left(V_i(t)/V_n - 1\right) \\ &+ 1/2\, Qd_i^n(t) \sum_y B_y \beta_y \left(\beta_y - 1\right)\left(V_i(t)/V_n - 1\right)^2 \end{aligned} \tag{11}$$

Equations (10) and (11) can be rewritten as follows based on (5).

$$\begin{aligned} Pd_i(V_i(t), y)/Pd_i^n(t) &= 1 + \sum_y A_y \alpha_y \left(V_i(t)/V_n - 1\right) \\ &+ 1/2 \sum_y A_y \alpha_y \left(\alpha_y - 1\right)\left(V_i(t)/V_n - 1\right)^2 \end{aligned} \tag{12}$$

$$\begin{aligned} Qd_i(V_i(t), y)/Qd_i^n(t) &= 1 + \sum_y B_y \beta_y \left(V_i(t)/V_n - 1\right) \\ &+ 1/2 \sum_y B_y \beta_y \left(\beta_y - 1\right)\left(V_i(t)/V_n - 1\right)^2 \end{aligned} \tag{13}$$

Expanding equations (12) and (13) leads to the derivation of the following expressions.

$$\begin{aligned} Pd_i(V_i(t), y)/Pd_i^n(t) &= 1/2 \sum_y A_y \alpha_y \left(\alpha_y - 1\right)\left(V_i(t)/V_n\right)^2 \\ &+ \sum_y A_y \alpha_y \left(2 - \alpha_y\right) V_i(t)/V_n + 1/2 \sum_y A_y \alpha_y \left(\alpha_y - 3\right) + 1 \end{aligned} \tag{14}$$

$$\begin{aligned} Qd_i(V_i(t), y)/Qd_i^n(t) &= 1/2 \sum_y B_y \beta_y \left(\beta_y - 1\right)\left(V_i(t)/V_n\right)^2 \\ &+ \sum_y B_y \beta_y \left(2 - \beta_y\right) V_i(t)/V_n + 1/2 \sum_y B_y \beta_y \left(\beta_y - 3\right) + 1 \end{aligned} \tag{15}$$

By using relations (16)–(21) to replace the multipliers of voltage terms in (14) and (15), equations (22) and (23) are obtained.

$$C_0 = 1 + 1/2 \sum_y A_y \alpha_y \left(\alpha_y - 3\right) \tag{16}$$

$$C_1 = \sum_y A_y \alpha_y \left(2 - \alpha_y\right) \tag{17}$$

$$C_2 = 1/2 \sum_y A_y \alpha_y \left(\alpha_y - 1\right) \tag{18}$$

$$D_0 = 1 + 1/2 \sum_y B_y \beta_y \left(\beta_y - 3\right) \tag{19}$$

$$D_1 = \sum_y B_y \beta_y \left(2 - \beta_y\right) \tag{20}$$

$$D_2 = 1/2 \sum_y B_y \beta_y \left(\beta_y - 1\right) \tag{21}$$

$$\begin{aligned} Pd_i(V_i(t), y)/Pd_i^n(t) &= C_2(y)\left(V_i(t)/V_n\right)^2 \\ &+ C_1(y)\left(V_i(t)/V_n\right) + C_0(y) \end{aligned} \tag{22}$$

$$\begin{aligned} Qd_i(V_i(t), y)/Qd_i^n(t) &= D_2(y)\left(V_i(t)/V_n\right)^2 \\ &+ D_1(y)\left(V_i(t)/V_n\right) + D_0(y) \end{aligned} \tag{23}$$

The summations for equations (16), (17), and (18), as well as equations (19), (20), and (21), can be expressed as follows:

$$\begin{aligned} C_0(y) + C_1(y) + C_2(y) &= 1 + 1/2 \sum_y A_y \alpha_y \left(\alpha_y - 3\right) \\ &+ \sum_y A_y \alpha_y \left(2 - \alpha_y\right) + 1/2 \sum_y A_y \alpha_y \left(\alpha_y - 1\right) \end{aligned} \tag{24}$$

$$\begin{aligned} D_0(y) + D_1(y) + D_2(y) &= 1 + 1/2 \sum_y B_y \beta_y \left(\beta_y - 3\right) \\ &+ \sum_y B_y \beta_y \left(2 - \beta_y\right) + 1/2 \sum_y B_y \beta_y \left(\beta_y - 1\right) = 0 \end{aligned} \tag{25}$$

Upon factoring A_y in equations (24) and (25), we obtain the following results:

$$\begin{aligned} &C_0(y) + C_1(y) + C_2(y) = 1 + \\ &1/2 \sum_y A_y \left(\alpha_y^2 - 3\alpha_y + 4\alpha_y - 2\alpha_y^2 + \alpha_y^2 - \alpha_y\right) \end{aligned} \tag{26}$$

$$\begin{aligned} &D_0(y) + D_1(y) + D_2(y) = 1 + \\ &1/2 \sum_y B_y \left(\beta_y^2 - 3\beta_y + 4\beta_y - 2\beta_y^2 + \beta_y^2 - \beta_y\right) \end{aligned} \tag{27}$$

Consequently:

$$C_0(y) + C_1(y) + C_2(y) = 1 + \sum_y A_y \left(\alpha_y^2 - \alpha_y^2 + 2\alpha_y - 2\alpha_y\right) \tag{28}$$

$$D_0(y) + D_1(y) + D_2(y) = 1 + \sum_y B_y \left(\beta_y^2 - \beta_y^2 + 2\beta_y - 2\beta_y\right) \tag{29}$$

Therefore, constraint (30) is obtained.

$$C_0(y) + C_1(y) + C_2(y) = D_0(y) + D_1(y) + D_2(y) = 1 \tag{30}$$

In (30), multipliers $C_0(y)$, $C_1(y)$, $C_2(y)$, $D_0(y)$, $D_1(y)$, and $D_2(y)$ are constant power, current, and impedance components of active and reactive load type y, respectively. Accordingly, equations (22), (23), and (30) represent quadratic models derived from (1) and (2), characterizing the association between load power, type, and voltage. The best solution strategy involves transforming the highly nonlinear exponential framework of equations (1) and (2) into a second-order model using (16)–(23). This approach is preferred due to the ease of handling equations (22) and (23) by commercial solvers compared to the difficulty with equations (1) and (2). Additionally, it allows for the potential calculation of load components from consumer type. Thus, per unit (pu) representation of (22) and (23) is as follows.

$$Pd_i(V_i(t), y) = Pd_i^n(t)\left(C_2(y)V_i^2(t) + C_1(y)V_i(t) + C_0(y)\right) \tag{31}$$

$$Qd_i(V_i(t), y) = Qd_i^n(t)\left(D_2(y)V_i^2(t) + D_1(y)V_i(t) + D_0(y)\right) \tag{32}$$

III. Creating a Model for Reconfiguration and Distributed Generators Accounting for the Impact of Time-Varying Power Demand and Load Type on Voltage

Aiming for the minimization of power losses (P_{Loss}), the reconfiguration problem in the presence of DGs can be formulated by (33) to (44).

$$Min\ P_{Loss} = \sum\nolimits_{ij\in\Omega^l} r_{ij} I_{ij}^{\ 2}(t) \tag{33}$$

subject to:

$$\begin{aligned} &Ps_i(t) + \sum\nolimits_{ki\in\Omega^l} P_{ki}(t) - \sum\nolimits_{ij\in\Omega^l} P_{ij}(t) - \sum\nolimits_{ij\in\Omega^l} r_{ij} I_{ij}^{\ 2}(t) + Pg_i(t) = \\ &Pd_i^n(t)\left(C_2(y)V_i^2(t) + C_1(y)V_i(t) + C_0(y)\right) \qquad \forall i \in \Omega^b \end{aligned} \tag{34}$$

$$\begin{aligned} &Qs_i(t) + \sum\nolimits_{ki\in\Omega^l} Q_{ki}(t) - \sum\nolimits_{ij\in\Omega^l} Q_{ij}(t) - \sum\nolimits_{ij\in\Omega^l} x_{ij} I_{ij}^{\ 2}(t) + Qg_i(t) \\ &= Qd_i^n\left(D_2(y)V_i^2(t) + D_1(y)V_i(t) + D_0(y)\right) \qquad \forall i \in \Omega^b \end{aligned} \tag{35}$$

$$\begin{aligned} &V_i^2(t) - V_j^{\ 2}(t) = 2\left[r_{ij}P_{ij}(t) + x_{ij}Q_{ij}(t)\right] + \left(r_{ij}^{\ 2} + x_{ij}^{\ 2}\right) I_{ij}^{\ 2}(t) + b_{ij}(t) \\ &\forall i \neq j \in \Omega^b,\ ij \in \Omega^l \end{aligned} \tag{36}$$

$$V_i(t) I_{ij}(t) = \sqrt{P_{ij}^{\ 2}(t) + Q_{ij}^{\ 2}(t)} \quad ij \in \Omega^l \tag{37}$$

$$V_{\min} \le V_i(t) \le V_{\max} \quad \forall i \in \Omega^b \tag{38}$$

$$0 \le I_{ij}(t) \le I_{ij}^{\max} y_{ij} \quad \forall ij \in \Omega^l \tag{39}$$

$$0 \le Pg_i(t) \le Pg_i^{\max} \quad \forall i \in \Omega^g \tag{40}$$

$$\left|b_{ij}(t)\right| \le \left(V_{\max}^2 - V_{\min}^2\right)\left(1 - y_{ij}\right) \qquad \forall ij \in \Omega^l \tag{41}$$

$$\begin{aligned} &-Ps_i(t)\tan(\operatorname{acos}(pfs_{lag})) \le Qs_i(t) \le Ps_i(t)\tan(\operatorname{acos}(pfs_{lead})) \\ &\forall i \in \Omega^s \end{aligned} \tag{42}$$

$$\left|Qg_i(t)\right| \le Pg_i(t)\tan(\cos^{-1}(pfg_i)) \quad \forall i \in \Omega^g \tag{43}$$

$$\sum\nolimits_{ij\in\Omega^l} y_{ij} = \left|\Omega^b\right| - 1 \tag{44}$$

where, sets Ω^l, Ω^b, Ω^s, and Ω^g consist of lines, system buses, substation and DG nodes, respectively. r_{ij} is the resistance and x_{ij} is the reactance of line ij. $Q_{ij}(t)$ and $P_{ij}(t)$ are reactive and active power flows through line ij at time t, respectively. $Qs_i(t)$ and $Ps_i(t)$ are substation's reactive and active powers, while $Qg_i(t)$, $Pg_i(t)$, and Pg_i^{max} are DG reactive and active power, and capacity at bus i and time t, respectively. $I_{ij}(t)$ is the magnitude of current in line ij and I_{ij}^{max} is its maximum amount at time t. V_{max} and V_{min} are the highest and lowest voltage magnitude of bus i. $b_{ij}(t)$ is a variable for indicating KVL at time t in the loop formed by line ij. y_{ij} is a binary number for representing the switch status within line ij. Furthermore, pfg_i is the DG power factor at bus i. pfs_{lag} and pfs_{lead} are the substation's lagging and leading power factors, respectively. The substation's lagging power factor defines the relationship between the reactive power consumption of the substation and its active power generation while the leading power factor determines the amount of reactive power injection of the substation according to its active power amount. Regarding the fact that substation should not consume the reactive power of distribution network, the lagging power factor is always considered to be zero in (42).

Equations (34) and (35) denote the balance between active and reactive power generation and consumption for each bus at time t. Equation (36) represents the cumulative voltage drop across all lines within a planar loop should be equal to zero in each time interval. Also, (37) relates active and reactive power flows to current and end bus voltage of each line in a time span. Constraints (38) and (39) represent momentary voltage and current limits, respectively. These constraints ensure that the voltage and current of each bus and line should not violet their permissible secure and thermal limits. (41) provides zero for $b_{ij}(t)$ in (36) if the switch of line ij is closed (y_{ij}=1) for the establishment of KVL in planar loops and gives a real number to $b_{ij}(t)$ when that switch is open (y_{ij}=0), i.e. KVL cannot be satisfied in loops including open branches. At each bus, (40) signifies that the active power generation of a DG is constrained by its active generation capacity because of inherent power generation limitation of each unit. Expression (42) illustrates the boundaries for the reactive power provision from the substation. This constraint indicates that the main network's reactive power should change in an interval depending on its active power generation. Constraint (43) indicates the thresholds for the reactive power generation and consumption capabilities of DG units. It means that DG units consume reactive power of the network or generate part of reactive power consumed by loads depending on their type, active power generation amount, and power factor. Equation (44) represents the condition of radial operation. Hence, in accordance with graph theory, the total count of operational branches must be equivalent to the total count of buses minus one. In this case, only tree structures of each distribution system is selected to show its radial operation. However, in large-sized distribution systems with more substations than 1 and grids including transfer nodes, (44) is unable to ensure radial topologies because reducing the number of all nodes ($|\Omega^b|$) by 1 is meaningful only in networks with one reference node (one substation). This constraint is not applicable if the number of substations is increased by one. Transfer nodes, i.e., buses without substation or demand, are frequently present in actual distribution grids. Hence, it is suggested to consider the adoption of efficient radiality constraints as follows in addition to (44).

$$y_{ij} = w_{ij} + w_{ji} \quad \forall ij \in \Omega^l \tag{45}$$

$$\sum\nolimits_{ij\in\Omega^l} w_{ij} = 1 \tag{46}$$

$$w_{ij} = 0 \quad \forall i \in \Omega^s,\ ij \in \Omega^l \tag{47}$$

$$w_{ji} = 0 \quad \forall j \in \Omega^s,\ ij \in \Omega^l \tag{48}$$

In (45)–(48), w_{ij} is a binary variable, indicating the direction of power in line ij. Equation (45) indicates that the power through a distribution branch of a radial system flows in one direction (no loop formation). w_{ij}=1 represents the direction of bus i towards j, whereas w_{ji}=1 indicates the opposite direction. It means that both omegas should be zero for an open switch (y_{ij}=0) because no power flow exists in open lines. On the other hand, if the switch will be closed (y_{ij}=1), one of the omegas should be 1 and another must be zero because in radial systems power flows through the line in a single direction. The model described by (33)–(44) is a challenging non-convex nonlinear optimization problem, marked by its non-convex nature, which is difficult to solve. For addressing this concern, quadratic voltage terms in (34) to (36) formulated as follows.

$$V_i^2(t) = \left(1 + V_i(t) - 1\right)^2 \tag{49}$$

Because of $\left| V_i(t)-1 \right| << 1$:

$$\left(1 + V_i(t) - 1\right)^2 \cong 1 + 2\left(V_i(t) - 1\right) = 2V_i(t) - 1 \tag{50}$$

Likewise, the non-convex and nonlinear equation (37) can be expressed in the following manner.

$$V_i^2(t) I_{ij}^2(t) \geq P_{ij}^2(t) + Q_{ij}^2(t) \qquad ij \in \Omega^l \tag{51}$$

Substituting $V_i^2(t)$ with (50) and $I_{ij}^2(t)$ with $\hat{I}_{ij}$, (51) can be formulated as

$$\left(2V_i(t) - 1\right)\hat{I}_{ij} \geq P_{ij}^2(t) + Q_{ij}^2(t) \tag{52}$$

Linear solvers cannot compute (52); hence, the subsequent variable transformation becomes imperative.

$$\tilde{V}_i(t) = 2V_i(t) - 1 \tag{53}$$

Consequently, the following equations can be employed to rewrite all expressions (34) to (38) in terms of linear representations of $\tilde{V}_i(t)$. Equation (54) has been obtained from (50) and (53).

$$V_i^2(t) = 2V_i(t) - 1 = \tilde{V}_i(t) \tag{54}$$

$$V_i(t) = 1/2\left(\tilde{V}_i(t) + 1\right) \tag{55}$$

To accommodate the new variable changes to (39), this linear constraint should be introduced as follows.

$$0 \leq I_{ij}^2(t) \leq \left(I_{ij}^{\max}\right)^2 y_{ij} \quad \forall ij \in \Omega^l \tag{56}$$

(56) is the square of (39). Furthermore, to enhance the computational efficiency of the model, the subsequent supplementary constraints should be integrated into the problem formulation. Although (39) is enough for keeping the power flows in its permissible limits, setting constraints (57) to (59) reduces the computational time due to more limited search space.

$$\left|P_{ij}(t)\right| \leq S_{ij}^{\max} y_{ij} \quad \forall ij \in \Omega^l \tag{57}$$

$$\left|Q_{ij}(t)\right| \leq S_{ij}^{\max} y_{ij} \quad \forall ij \in \Omega^l \tag{58}$$

$$S_{ij}^{\max} = V_{\max} I_{ij}^{\max} \qquad \forall ij \in \Omega^l \tag{59}$$

Within the aforementioned relationships, $S_{ij}^{\max}$ denotes the maximum magnitude of complex power in line *ij*. Likewise, the substation must refrain from consuming reactive power from the grid; thus, psf_{lag} is assigned a value of 1. Through the substitution of (54) and (55) and $I_{ij}^2(t)=\hat{I}_{ij}$ in (33)–(36) and (56), and (52) and (53) in (37), and incorporating (45)–(48), (57)–(59) and limits on reactive power of DG into (33)–(44), a mixed-integer programming model that combines reconfiguration and DG operation is proposed as follows for increased efficiency.

$$Min\ P_{Loss} = \sum\nolimits_{ij \in \Omega^l} r_{ij} \hat{I}_{ij}(t) \tag{60}$$

S.t.:

$$\begin{aligned} &Ps_i(t) + \sum\nolimits_{ki \in \Omega^l} P_{ki}(t) - \sum\nolimits_{ij \in \Omega^l} P_{ij}(t) - \sum\nolimits_{ij \in \Omega^l} r_{ij}\hat{I}_{ij}(t) + Pg_i(t) = \\ &Pd_i^n(t)\left(C_2(y)\tilde{V}_i(t) + 1/2\,C_1(y)\left(\tilde{V}_i(t)+1\right) + C_0(y)\right) \qquad \forall i \in \Omega^b \end{aligned} \tag{61}$$

$$\begin{aligned} &Qs_i(t) + \sum\nolimits_{ki \in \Omega^l} Q_{ki}(t) - \sum\nolimits_{ij \in \Omega^l} Q_{ij}(t) - \sum\nolimits_{ij \in \Omega^l} x_{ij}\hat{I}_{ij}(t) + Qg_i(t) \\ &= Qd_i^n(t)\left(D_2(y)\tilde{V}_i(t) + 1/2\,D_1(y)\left(\tilde{V}_i(t)+1\right) + D_0(y)\right) \quad \forall i \in \Omega^b \end{aligned} \tag{62}$$

$$\begin{aligned} &\tilde{V}_i(t) - \tilde{V}_j(t) = 2\left[r_{ij}P_{ij}(t) + x_{ij}Q_{ij}(t)\right] + \left(r_{ij}^2 + x_{ij}^2\right)\hat{I}_{ij}(t) + b_{ij}(t) \\ &\forall i \neq j \in \Omega^b, ij \in \Omega^l \end{aligned} \tag{63}$$

$$\tilde{V}_i(t)\hat{I}_{ij}(t) \geq P_{ij}^2(t) + Q_{ij}^2(t) \tag{64}$$

$$V_{\min} \leq 1/2\left(\tilde{V}_i(t)+1\right) \leq V_{\max} \quad \forall i \in \Omega^b \tag{65}$$

$$0 \leq \hat{I}_{ij}(t) \leq \left(I_{ij}^{\max}\right)^2 y_{ij} \quad \forall ij \in \Omega^l \tag{66}$$

$$\left|b_{ij}(t)\right| \leq 2\left(V_{\max} - V_{\min}\right)\left(1 - y_{ij}\right) \quad \forall ij \in \Omega^l \tag{67}$$

$$0 \leq Pg_i(t) \leq Pg_i^{\max} \quad \forall i \in \Omega^g \tag{68}$$

$$Qg_i^{\min} \leq Qg_i(t) \leq Qg_i^{\max} \quad \forall i \in \Omega^g \tag{69}$$

$$0 \leq Qs_i(t) \leq Ps_i(t)\tan(\cos^{-1}(pfs_{lead})) \quad \forall i \in \Omega^s \tag{70}$$

$$\begin{aligned} &-Pg_i(t)\tan(\cos^{-1}(pfg_i)) \leq Qg_i(t) \leq Pg_i(t)\tan(\cos^{-1}(pfg_i)) \\ &\forall i \in \Omega^g \end{aligned} \tag{71}$$

$$\sum\nolimits_{ij \in \Omega^l} y_{ij} = \left|\Omega^b\right| - \left|\Omega^s\right| \tag{72}$$

$$y_{ij} = w_{ij} + w_{ji} \quad \forall ij \in \Omega^l \tag{73}$$

$$\sum\nolimits_{ij \in \Omega^l} w_{ij} = 1 \tag{74}$$

$$w_{ij} = 0 \quad \forall i \in \Omega^s, ij \in \Omega^l \tag{75}$$

$$w_{ji} = 0 \quad \forall j \in \Omega^s, ij \in \Omega^l \tag{76}$$

$$-V_{\max} I_{ij}^{\max} y_{ij} \leq P_{ij}(t) \leq V_{\max} I_{ij}^{\max} y_{ij} \quad \forall ij \in \Omega^l \tag{77}$$

$$-V_{\max} I_{ij}^{\max} y_{ij} \leq Q_{ij}(t) \leq V_{\max} I_{ij}^{\max} y_{ij} \quad \forall ij \in \Omega^l \tag{78}$$

In (69), Qg_i^{min} and Qg_i^{max} represent the lowest and highest level of DG's reactive generation at bus *i*.

IV. Simulation Results

The proposed model, formulated as a convex mixed-integer programming problem, can be effectively solved using linear solvers. For this study, the CPLEX in AMPL is employed to optimize the model established in equations (60) to (78) using a 3.6-GHz and 8-GB RAM processor. To demonstrate the efficacy of our proposed reconfiguration and DG operation model, the formulation was tested on 33- and 69-bus distribution systems, shown in Figs 1 and 2, using the actual hourly load profile of the Regional Electric Company of Tehran (RECT) [20], and the results were compared with some other existing models and methods. Dashed and solid lines in figures exhibit tie and sectional switches, respectively.

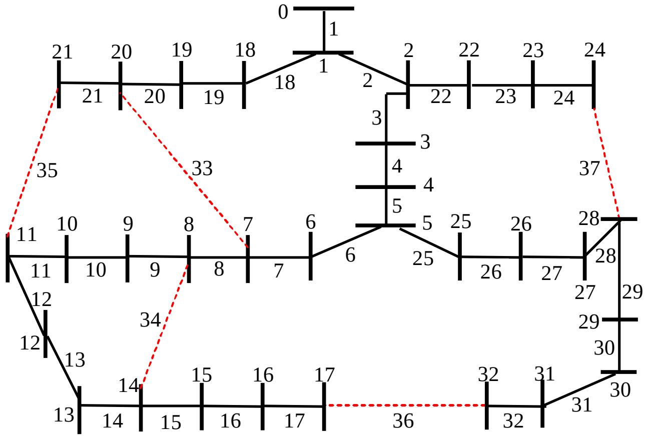

Figure 1. Initial topology of the 33-bus disitbution grid.

It is important to note that Qg_i^{min}, Qg_i^{max}, and pfs_{lead} are considered 0, 1000 kVAr, and 0.8, respectively. The data of both test systems are available in [21] and [22]. The proposed formulation was examined in different cases of DG arrangement, and the results are presented in Tables II and III. Table I lists the DG capacities and their corresponding locations in each test system. To ensure a precise comparison between our outcomes and those presented in [15], the identical load components as utilized in [15] were adopted for composite load simulation.

Table I presents cases for each test system, featuring diverse capacities and locations of DGs. This presentation aims to validate and corroborate the method's efficacy across a range of scenarios.

Table II presents results in a scenario with DG operation along with the reconfiguration problem for the 33-bus system. In this table, constant current loads are consumers whose power demand is varied as linear by grid's voltage, while the amount of constant impedance loads is changed with the square of the voltage. The proposed solution suggests the same switching combination as the one provided by TLBO [6], ICA [23], MIQP [7], MISOCP [24], and GA [10] when constant power is assumed for all load models. In other cases, the proposed approach has provided different configurations than the ones presented by the literature, which also diverge from each other. In particular, the configuration results for Case 3 in the 33-bus system present a significant change in the network configuration. Even though presenting different configurations, the proposed method obtained smaller levels of power losses compared to other methodologies.

Tables II and III revealed that, in the case of both test systems, the proposed model produced configurations different from those outlined in the existing literature and also with improved results. The rapidity of the solution becomes apparent when contrasted with the time demands of the models introduced in the existing literature which the proposed model is compared to.

TABLE I. DG CHARACTERISTICS OF THE CASE STUDY SYSTEMS

Test Systems	Cases	Bus	Active power (kW)	Power factor
33-bus	Case 1 [6]	3	50	0.8
		6	100	0.9
		24	200	0.9
		29	100	1
	Case 2 [7]	10	800	0.848
	Case 3 [9]	24	150	0.9
	Case 4 [10]	4	50	0.8
		7	100	0.9
		25	200	0.9
		30	100	1
	Case 5 [15]	9	280	1
		13	280	1
		25	280	1
		30	280	1
69-bus	Normal	21	300	1
		33	100	1
		46	200	1
		62	400	1
	Light	59	4000	0.95

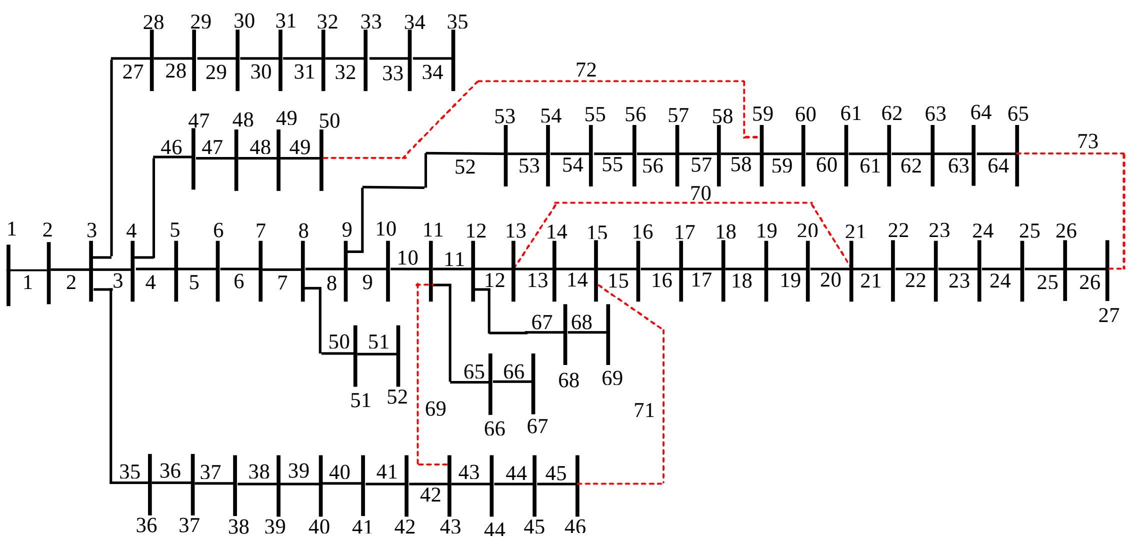

Figure 2. Initial topology of the 69-bus disitbution grid.

TABLE II. RESULTS AFTER SIMULTANEOUS RECONFIGURATION AND DG PLANNING IN THE 33-BUS SYSTEM

Case	Method/Model	Load type/component	Power loss (kW)				Best solution		Minimum voltage (pu)
			Best	Worst	Mean	Standard deviation	Open lines/switches	CPU time (s)	
1	TLBO [6]	Constant power	115.70	117.20	115.90	-	7,9,14,28,32	8	0.9489
	ICA [23]		115.70	118.50	116.10	-	7,9,14,28,32	6	0.9489
	Proposed	**Constant power**	115.70	115.70	115.70	0	7,9,14,28,32	0.96	0.9489
		Constant current	106.06	106.06	106.06	0	7,9,14,28,32	1.39	0.9510
		Constant impedance	97.58	97.58	97.58	0	7,9,14,28,32	1.58	0.9530
2	MIQP [7]	Constant power	95.27	95.27	95.27	0	6,8,14,21,37	3.63	0.9459
	MISOCP [24]		95.27	95.27	95.27	0	6,8,14,21,37	6.1	0.9459
	Proposed	**Constant power**	86.33	86.33	86.33	0	6,8,14,35,37	0.98	0.9757
		Constant current	84.09	84.09	84.09	0	6,8,14,35,37	2.13	0.9770
		Constant impedance	82.22	82.22	82.22	0	6,8,14,35,37	2.85	0.9782
3	WOA [9]	Constant power	138.21	-	-	0.0114	10,28,33,34,36	109.13	0.9348
	AWOA [9]		138.96	-	-	0.0106	10,28,33,34,36	105.45	0.9358
	PSO [9]		136.54	-	-	0.0151	13,28,33,34,36	112.07	0.9378
	GWO [9]		134.13	-	-	0.0125	10,28,33,34,36	106.43	0.9378
	PSMA [9]		133.38	-	-	0.0060	10,28,33,34,36	92.74	0.9420
	Proposed	**Constant power**	129.92	129.92	129.92	0	7,9,14,28,32	1.23	0.9455
		Constant current	119.06	119.06	119.06	0	7,9,14,28,32	1.38	0.9480
		Constant impedance	109.52	109.52	109.52	0	7,9,14,28,32	0.85	0.9503
4	GA [10]	Constant power	112	-	-	-	7,9,14,28,32	-	0.9455
	AS [10]		129.50	-	-	-	6,9,14,26,31	-	0.9231
	ACO [10]		118.17	-	-	-	6,10,14,17,28	-	0.9435
	Proposed	**Constant power**	111.43	111.43	111.43	0	7,9,14,28,32	1.13	0.9455
		Constant current	102.24	102.24	102.24	0	7,9,14,28,32	1.44	0.9510
		Constant impedance	94.15	94.15	94.15	0	7,9,14,28,32	1.25	0.9530
5	GWO [15]	Composite	82.91	-	-	0.0317	7,10,14,28,32	2.54	0.9500
	Proposed	**Composite**	77.01	77.01	77.01	0	7,10,13,30,37	1.11	0.9504
		Constant power	85.44	83.99	83.99	0	7,10,13,32,37	1.34	0.9551
		Constant current	77.19	77.19	77.19	0	7,10,13,30,37	1.52	0.9503
		Constant impedance	71.42	71.42	71.42	0	7,10,13,30,37	1.80	0.9535

TABLE III. SIMULTANEOUS RECONFIGURATION AND DG PLANNING RESULTS IN THE 69-BUS SYSTEM

Load amount	Method/Model	Load type/component	Power loss (kW)			Best solution		Minimum voltage (pu)
			Best	Worst	Mean	Open lines/switches	CPU time (s)	
Normal	TLBO [6]	Constant power	67.75	69.6	68.3	12,57,63,69,70	140	0.9520
	ICA [23]		67.79	68.9	68.7	14,57,63,69,70	632	0.9520
	Proposed	**Constant power**	67.70	67.70	67.70	12,57,62,69,70	5.39	0.9520
		Constant current	61.85	61.85	61.85	12,55,63,69,70	12.31	0.9545
		Constant impedance	56.80	56.80	56.80	12,58,62,69,70	21.81	0.9567
Light	MILP [12]	Constant current	13.88	13.88	13.88	12,55,64,69,70	-	0.9689
	Proposed	**Constant current**	12.87	12.87	12.87	12,53,64,69,70	4.58	0.9761
		Constant power	13.35	13.35	13.35	12,53,64,69,70	3.08	0.9764
		Constant impedance	12.39	12.39	12.39	12,53,64,69,70	4.20	0.9759

In a scenario involving constant power, the proposed method delivered a solution that was over 90 times quicker than the PSO approach in Case 3 of the 33-bus system. Additionally, it was more than 117 times faster than the ICA method under normal load conditions within the 69-bus system. As anticipated, across all cases and for both systems, the scenario characterized by pure constant impedance load models emerges as the configuration resulting in the least power losses within the system. A further noteworthy advantage of the presented method is its precision. In contrast, the methodologies outlined in the literature solely incorporate constant power load models, exhibiting standard deviations for worst and best power losses that vary from 0.006 (PSMA) to 0.0317 (GWO). In the 33-bus test system, both MIQP and MISOCP were capable of delivering zero standard deviation. Nonetheless, the proposed model demonstrated robustness by achieving no deviation for both test systems in any load type. The only limitation of the proposed method is its lower accuracy for distribution systems with high voltage variations.

V. CONCLUSION

The reconfiguration of distribution grids as an established method for minimizing active power losses, has been thoroughly investigated by academia and extensively implemented by utilities. In addition to this, distributed generators (DGs) allocation can also play a substantial role in aiding power loss minimization. Given the increasing integration of distributed energy resources, the hybrid utilization of reconfiguration and DGs stands out as a highly effective approach for curtailing power losses within distribution systems. Customers' load consists of various types that their demands vary with voltage levels and time, in line with consumption patterns. Also, as a majority of loads exhibit voltage-dependent characteristics, fluctuations in load power also exert an impact on the system's voltages and power losses. Hence, alterations in system voltage could potentially affect the suggested radial topologies utilized for grid reconfiguration. While a small number of papers have addressed voltage-dependent load models, the majority of research pertaining to grid reconfiguration and DG planning has disregarded this factor due to its nonlinear nature and the associated extensive computational time.

This study introduced a streamlined model to address distribution grid reconfiguration challenges, encompassing DG allocation alongside voltage-dependent and time-varying loads. The problem was transformed into a convex mixed-integer programming formulation, presenting a sufficiently straightforward model suitable for implementation within conventional optimization tools. This model can then be effectively resolved using commercial linear solvers. Through its avoidance of extensive linearization and approximation, the model delivers both rapidness and precision in identifying appropriate solutions for the joint simultaneous grid reconfiguration and DG planning. The effectiveness of the proposed method was demonstrated in two different test distribution grids, and the outcomes were compared with approaches suggested in existing literature. Based on the numerical findings derived from the 33- and 69-bus distribution systems, the configurations proposed are different and depend on the composition of load type even when the DGs' generation level and location remain consistent. The comparison of results revealed that the proposed model not only managed to curtail active power losses and enhance the system's minimum voltage, but it also offered solutions within a shorter computational duration, while upholding the accuracy of the results. In addition to its fastness, another key advantage of the proposed method is its robustness, as evidenced by the attainment of zero standard deviation for both the best and worst case scenario in constant impedance, current, and power load models.

REFERENCES

[1] M. Mahdavi, M. S. Javadi, and J. P. S. Catalão, "Integrated generation-transmission expansion planning considering power system reliability and optimal maintenance activities," *Int. J. Electr. Power & Energy Syst.*, vol. 145, pp. 1-21, 2023.

[2] M. Mahdavi, M. S. Javadi, F. Wang, and J. P. S. Catalão, "An efficient model for accurate evaluation of consumption pattern in distribution system reconfiguration," *IEEE Trans. Ind. App.*, vol. 58, no. 3, pp. 3102-3111, 2022.

[3] M. Mahdavi, H. H. Alhelou, P. Siano, and V. Loia, "Robust mixed-integer programing model for reconfiguration of distribution feeders under uncertain and variable loads considering capacitor banks, voltage regulators, and protective relays," *IEEE Trans. Ind. Informat.*, vol. 18, no. 11, pp. 7790-7803, 2022.

[4] M. Mahdavi, M. Javadi, F. Wang, and J. P. S. Catalão, "An accurate evaluation of consumption pattern in reconfiguration of electrical energy distribution systems," in *Proc. 2021 IEEE Ind. Appl. Soc. An. Meet.*, Vancouver, Canada, 2021, pp. 1-7.

[5] Z. Ye, C. Chen, B. Chen, and K. Wu, "Resilient service restoration for unbalanced distribution systems with distributed energy resources by leveraging mobile generators," *IEEE Trans. Ind. Informat.*, vol. 17, no. 2, pp. 1386-1396, 2021.

[6] A. Lotfipour and H. Afrakhte, "A discrete Teaching–Learning-Based Optimization algorithm to solve distribution system reconfiguration in presence of distributed generation," *Int. J. Electr. Power & Energy Syst.*, vol. 82, pp. 264-273, 2016.

[7] T. Yang, Y. Guo, L. Deng, H. Sun, and W. Wu, "A linear branch flow model for radial distribution networks and its application to reactive power optimization and network reconfiguration," *IEEE Trans. Smart Grid*, vol. 12, no. 3, pp. 2027-2036, 2021.

[8] T. H. B. Huy, T. V. Tran, D. N. Vo, and H. T. T. Nguyen, "An improved metaheuristic method for simultaneous network reconfiguration and distributed generation allocation," *Alexandria Eng. J.*, vol. 61, pp. 8069-8088, 2022.

[9] H.-J. Wang, J.-S. Pan, T.-T. Nguyen, and S. Weng, "Distribution network reconfiguration with distributed generation based on parallel slime mould algorithm," *Energy*, vol. 244, no. 123011, pp. 1-19, 2022.

[10] Y. K. Wu, C. Y. Lee, L. C. Liu, and S. H. Tsai, "Study of reconfiguration for the distribution system with distributed generators," *IEEE Trans. Power Del.*, vol. 5, pp. 1678-1685, 2010.

[11] E. Azad-Farsani, I. Goroohi Sardou, and S. Abedini, "Distribution network reconfiguration based on LMP at DG connected busses using game theory and self-adaptive FWA," *Energy*, vol. 215, pp. 1-11, 2021.

[12] J. F. Franco, M. J. Rider, M. Lavorato, and R. Romero, "A mixed-integer LP model for the reconfiguration of radial electric distribution systems considering distributed generation," *Electr. Power Syst. Res.*, vol. 97, pp. 51-60, 2013.

[13] E. Dall'Anese and G. B. Giannakis, "Sparsity-leveraging reconfiguration of smart distribution systems," *IEEE Trans. Power Del.*, vol. 29, no. 3, pp. 1417-1426, 2014.

[14] H. R. Esmaeilian and R. Fadaeinedjad, "Energy loss minimization in distribution systems utilizing an enhanced reconfiguration method integrating distributed generation," *IEEE Syst. J.*, vol. 9, no. 4, pp. 1430-1439, 2015.

[15] V. B. Pamshetti, S. Singh, and S. P. Singh, "Combined impact of network reconfiguration and volt-VAR control devices on energy savings in the presence of distributed generation," *IEEE Syst. J.*, vol. 14, no. 1, pp. 995-1006, 2020.

[16] M. Mahdavi, A. Kimiyaghalam, H. H. Alhelou, M. S. Javadi, A. Ashouri, and J. P. S. Catalão, "Transmission expansion planning considering power losses, expansion of substations and uncertainty in fuel price using discrete artificial bee colony algorithm," *IEEE Access*, vol. 9, pp. 135983-135995, 2021.

[17] X. Qiao, Y. Luo, J. Xiao, Y. Li, L. Jiang, X. Shao, J. Xu, Y. Tan, and Y. Cao, "Optimal scheduling of distribution network incorporating topology reconfiguration, BES and load response: A MILP model," *CSEE J. Power and Energy Syst.*, vol. 8., no. 3, pp. 743-756, 2022.

[18] M. A. Mejia, L. H. Macedo, G. Muñoz-Delgado, J. Contreras, and A. Padilha-Feltrin, "Medium-term planning of active distribution systems considering voltage-dependent loads, network reconfiguration, and CO_2 emissions," *Int. J. Electr. Power Energy Syst.*, vol. 135, pp. 1-14, 2022.

[19] L. M. Korunovic, S. Sterpu, S. Djokic, K. Yamashita, S. M. Villanueva, and J. V. Milanovic, "Processing of load parameters based on existing load models," in *Proc. 3rd IEEE Power Energy Soc. Innovative Smart Grid Technol. Eur.*, Berlin, Germany, 2012, pp. 1-6.

[20] M. Mahdavi, C. Sabillón, M. Ajalli, H. Monsef, and R. Romero, "A real test system for power system planning, operation, and reliability," *J. Control Autom. Electr. Syst.*, vol. 29, pp. 192-208, 2018.

[21] M. E. Baran and F. F. Wu, "Network reconfiguration in distribution systems for loss reduction and load balancing," *IEEE Trans. Power Del.*, vol. 4, no. 2, pp. 1401-1407, 1989.

[22] C. Sahoo and K. Prasad, "A fuzzy genetic approach for network reconfiguration to enhance voltage stability in radial distribution systems," *Energy Convers. Manag.*, vol. 47, pp. 3288-3306, 2006.

[23] S. H. Mirhoseini, S. M. Hosseini, M. Ghanbari, and M. Ahmadi, "A new improved adaptive imperialist competitive algorithm to solve the reconfiguration problem of distribution systems for loss reduction and voltage profile improvement," *Int. J. Electr. Power & Energy Syst.*, vol. 55, pp. 128-143, 2014.

[24] Z. Tian, W. Wu, B. Zhang, and A. Bose, "Mixed-integer second-order cone programing model for VAR optimisation and network reconfiguration in active distribution networks," *IET Gener. Transm. Distrib.*, vol. 10, no. 8, pp. 1938-1946, 2016.